

## **Three-Dimensional Finite Element Analysis of Adhesively Bonded Single Lap Joints in Laminated FRP Composites Subjected to Thermal Loading With C-C End Conditions**

**M. Venkateswara Rao<sup>1</sup>, K. Mohana Rao<sup>2</sup>, V. Rama Chandra Raju<sup>3</sup>,  
V. Bala Krishna Murthy<sup>4</sup> and V.V. Sridhara Raju<sup>4</sup>**

<sup>1</sup>*Mechanical Engineering Department, Bapatla Engineering College,  
Bapatla, A.P, India.*

*Email: mvr2007rao@rediffmail.com*

<sup>2</sup>*K.L. College of Engineering, Vaddeswaram, A.P., India.*

<sup>3</sup>*J.N.T. University, Vizayanagaram, A.P., India.*

<sup>4</sup>*Mech. Engg. Department, P. V. P. Siddhartha Institute of Technology,  
Vijayawada, A.P, India.*

### **Abstract**

The present investigation deals with the thermo-elastic analysis of adhesively bonded single lap joint in laminated FRP composites using three-dimensional theory of elasticity based finite element method. The finite element model is validated with the available results in the literature for the longitudinal loading of a single lap joint (SLJ) made of specially orthotropic laminates and is extended for the analysis of a single lap joint made of generally orthotropic laminates subjected to non-linear temperature loads. The out-of-plane normal and shear stresses are computed at the interfaces of the adherends and adhesive, and at mid surface of the adhesive. The results of the present analysis reveals that the three-dimensional stress analysis is required for the analysis of single lap joint in laminated FRP composites.

**Key words:** SLJ, FEM, FRP, Interlaminar stresses

### **Introduction**

Fiber reinforced plastic (FRP) materials have proven to be very successful in structural applications. They are widely used in the aerospace, automotive and marine industries. FRP materials or composites behave differently than typical metals such as

steel or aluminum. A typical composite contains layers of aligned fibers oriented at different angles held together by a resin matrix, giving high strength and stiffness in different directions. This anisotropy can cause difficulties when joining two parts together, especially if the two pieces have different stiffness and strength characteristics. The joint can potentially become the weakest link in the structure due to the large amount of load it must transfer. There are wide varieties of ways to join different parts together. Two major methods include mechanical fastening and adhesive bonding. Adhesive bonding of structures has significant advantages over conventional fastening systems. Bonded joints are considerably more fatigue resistant than mechanically fastened structures because of the absence of stress concentrations that occur at fasteners. Joints may be lighter due to the absence of fastener hardware. A major advantage of adhesive bonds is that adhesive bonds may be designed and made in such a way that they can be stronger than the ultimate strength of many metals in common use for aircraft construction.

The stresses induced at the interfaces of the adherends and adhesive play an important role in the design of adhesively bonded joints in FRP composites. Hence, these stresses are required to be analyzed most accurately.

In 1938, Volkersen [1] first proposed a simple shear lag model for mechanical joints with many fasteners, and later on, this model was adopted for adhesively bonded lap joints with the assumption that the adherends are in tension and adhesive is in shear only and both stresses are constant across the thickness. In 1944, Goland and Reissner [2] took into consideration the effects of the adherends bending and the peel stress, as well as the shear stress, in the adhesive layer in a single lap joint. Subsequent efforts by Oplinger [3] suggested the corrections to the Goland and Reissner solution by using a layered beam theory instead of classical homogeneous beam model for single lap joints. The corrections in the shear lag model, or Volkersen solution, include works by Hart-Smith [4,5] and Tsai et.al [6]. Hart-Smith [4,5] modified the shear lag model to include the adhesive plasticity. Tsai et.al [6] provided a correction to the shear lag model with the assumption that the shear stress is linear through the adherends. The analysis of Klarbring and Movchan [7] involved mathematically modeling the adhesive joint using an asymptotic approach. Kim and Kedward [8] used finite difference method for the analysis of adhesively bonded joints. Penado and Dropek [9] and Tessler et.al [10] used finite element method for the analysis of adhesively bonded joints.

Adams and Peppiatte [11] analyzed a bonded joint using a two dimensional linear elastic finite element method with plane strain assumption. Examples of finite element investigations of adhesively bonded composite joints include Kairouz and Matthews [12], Tong [13], Li et al. [14]. Delale et al. [15] developed a closed-form solution for lap-shear joints with orthotropic adherends using classical plate theory. Mortensen [16] presented a unified analytical approach to analyze an array of common bonded joint configurations for more general loading conditions. Panigrahi and Pradhan [17] studied; a single lap joint with the adherends made of specially orthotropic laminates for the evaluation of the tri-axial stress field using finite element analysis and proved the necessity of three-dimensional stress analysis of single lap joint. Venkateswara Rao et al analyzed a single lap joint in FRP composites subjected to axial and

transverse pressure loads with adherends made of generally orthotropic laminates [18,19].

The objective of the present paper is to extend the three-dimensional stress analysis of Venkateswara Rao et al [18] for the single lap joint subjected to non-linear temperature distribution. The analysis includes the evaluation of i) Interlaminar normal stress ( $\sigma_{zz}$ ), ii) Interlaminar shear stress in longitudinal plane ( $\tau_{zx}$ ) and iii) Interlaminar shear stress in transverse plane ( $\tau_{yz}$ ) at the interfaces of the adherends and adhesive, and at the middle plane of the adhesive.

## Problem Modeling

### Geometry

The geometry of the problem for longitudinal loading (used for the validation purpose) is as shown in Fig. 1. In case of transverse loading, the thickness of the adherends is increased to maintain the length-to-thickness ratio ( $s$ ) equal to 10. The thickness of the adhesive is increased proportionately with the thickness of the adherends. The in-plane dimensions for the transverse loading are same as that of longitudinal loading.

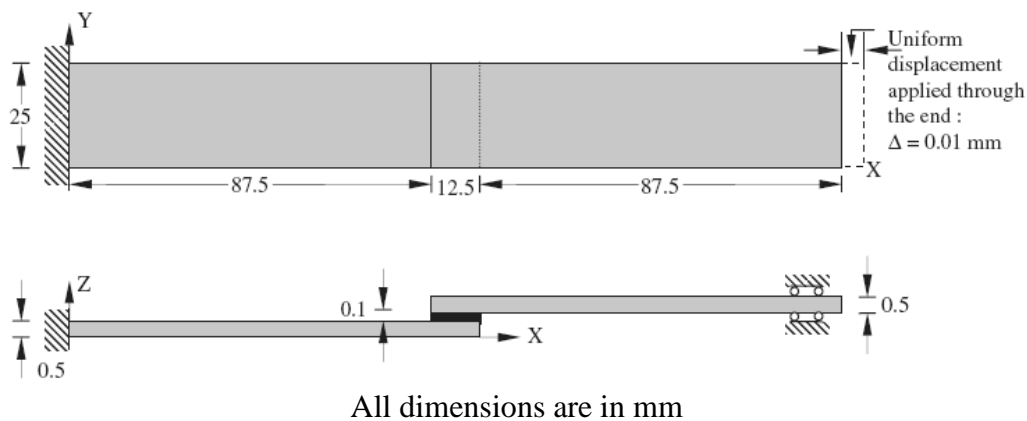


**Figure 1:** Geometry of the single lap joint.

### Finite Element Model

The finite element mesh is generated using a three-dimensional brick element 'SOLID 45' of ANSYS [18]. This element (Fig. 2) is a structural solid element designed based on three-dimensional elasticity theory and is used to model thick orthotropic solids. The element is defined by 8 nodes having three degrees of freedom per node: translations in the nodal x, y, and z directions.

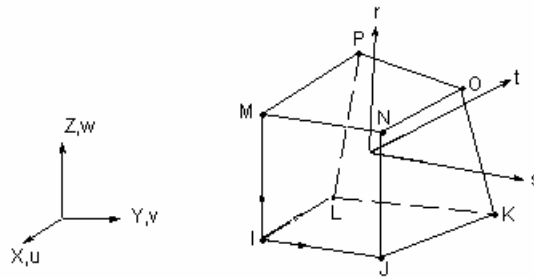


**Figure 2:** SOLID 45 Element.

### Loading

The following types of loads are applied for validation and prediction of the response of the structure for the present analysis.

- (i) A uniform longitudinal displacement of 0.01 mm for the validation purpose.
- (ii) A non-linear temperature load obtained from thermal analysis with following conditions:
  - $100^{\circ}\text{C}$  on top surface of the joint
  - Convection at bottom and side faces of the joint with  $h = 5 \text{ W/m}^2\text{K}$  and  $T_{\infty} = 30^{\circ}$ .
  - Insulation at the fixed ends of the joint

### Boundary Conditions

Both the ends of the joint are clamped (C-C) i.e. all the degrees of freedom (x-, y- and z-) are constrained at both the ends.

### Material Properties

The following mechanical properties are taken for the thermoelastic analysis of single lap joint.

#### i) Epoxy (adhesive)

$$E = 5.171 \text{ GPa}; \quad \nu = 0.35; \quad k = 0.18 \text{ W/m K}; \quad \alpha = 72\text{e-}6/^{\circ}\text{C}$$

#### ii) Graphite-Epoxy (adherends)

$$\begin{aligned} K_L &= 36.42 \text{ W/m K} & K_T &= 0.96 \text{ W/m K} \\ E_1 &= 172.72 \text{ GPa}, & E_2 &= E_3 = 6.909 \text{ GPa} \\ G_{12} &= G_{13} = 3.45 \text{ GPa}, & G_{23} &= 1.38 \text{ GPa}, & \nu_{12} &= \nu_{13} = \nu_{23} = 0.25 \\ \alpha_1 &= 0.57 \times 10^{-6}/^{\circ}\text{C} & \alpha_2 &= \alpha_3 = 35.6 \times 10^{-6}/^{\circ}\text{C} \end{aligned}$$

### Laminate sequence

- (i) Two  $0^{\circ}/90^{\circ}/90^{\circ}/0^{\circ}$  laminated FRP composite plates are used as adherends for the validation of present FE model with reference [17].

- (ii) Two  $+\theta^0/-\theta^0/-\theta^0/+ \theta^0$  laminated FRP composite plates are used as adherends for the present analysis. The value of  $\theta$  is measured from the longitudinal direction of the structure (x-axis) and varied from  $0^0$  to  $90^0$  in steps of  $15^0$ .

**Results**

**Validation**

Fig. 3 shows the finite element mesh on the overlap region of the single lap joint. The present finite element model is validated by comparing the stresses obtained for the single lap joint of specially orthotropic laminates with the results of reference [17] for longitudinal loading. Table. 1 shows the comparison of maximum values of the stresses at the specified locations and close agreement is found. Later this model is extended for the analysis of single lap joint of generally orthotropic laminates subjected to non-linear temperature loading.

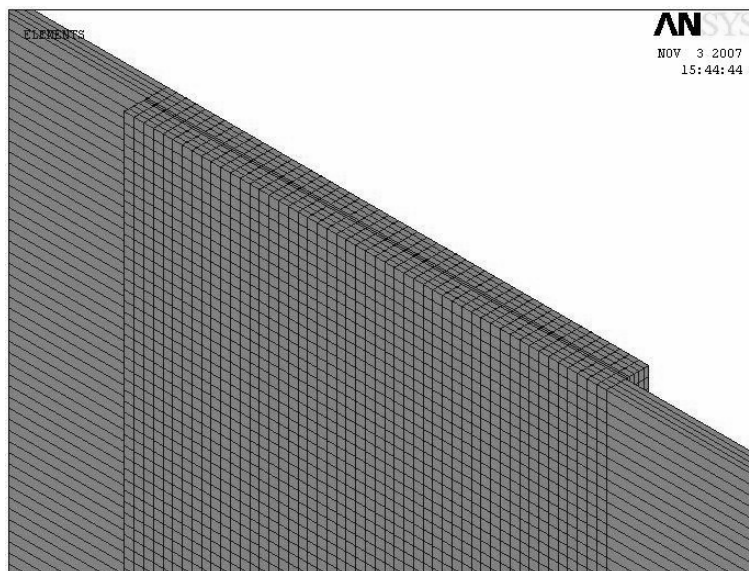


**Figure 3:** Finite element mesh on the overlap region of the single lap joint.

**Table 1:** Validation of the finite element model.

Location	$\sigma_{zz}$ (MPa)		$\tau_{yz}$ (MPa)		$\tau_{zx}$ (MPa)	
	Ref [17]	Present	Ref [17]	Present	Ref [17]	Present
Top Interface	0.40	0.41	0.08	0.14	0.39	0.40
Bottom Interface	0.39	0.39	0.08	0.13	0.38	0.39

### Variation of the stresses across the width of the laminate

One of the reasons for the variation of the stresses across the width of the laminate is due to the non-uniform arrangement of the fibers in the width direction except at  $\theta = 0^\circ$  and  $90^\circ$ . The second reason is due to the coupling between bending, shear, and extensions in the deformations of the laminates. Another reason is due to the interlaminar effect at the free edges of the structure.

Fig. 4 illustrates the variation of normal stress  $\sigma_{zz}$  for several fiber angles  $\theta$  across the width of the structure. The normal stress for  $\theta=0^\circ$  is maximum at the ends of the joint and zero at  $y=2\text{mm}$ , later increases and flat between 3 mm and 22.5mm followed by rapid rise between 22.5mm and 25mm. This stress for  $\theta=30^\circ$  is positive between 0mm and 2 mm and negative between 2mm and 21mm, later increases sharply with maximum value at  $y=25\text{mm}$ . For  $\theta=45^\circ$ , positive stress value is observed up to 1mm, negative stress between 1mm and 21mm, later increases sharply with maximum value at  $y=25\text{mm}$ . For  $\theta=60^\circ$ , the negative value increases up to 5mm, later decreases and turns to positive value at 22.5mm followed by increase of stress. For  $\theta=30^\circ, 45^\circ$  and  $60^\circ$ , the maximum stress value is noticed at  $y=25\text{mm}$ . For  $\theta=90^\circ$ , this stress is constant between 5mm and 20mm later increase of stress followed by slight drop in stress at both the ends of the joint.

The non-linear variation of Shear Stress  $\tau_{yz}$ , for several fiber angles  $\theta$  across the width is shown in Fig.5. The Shear Stress for  $\theta=0^\circ, 60^\circ$  and  $90^\circ$  is positive and maximum at one end i.e. at  $y=0\text{mm}$ , zero at the middle i.e. at  $y=12.5\text{mm}$  and then turns to negative beyond 12.5mm with negative maximum at  $y=25\text{mm}$ . This Stress for  $\theta = 30^\circ$  and  $45^\circ$  is positive and maximum at  $y=0\text{mm}$ , decreasing gradually and changed to negative between  $y=5\text{mm}$  and 10mm with negative maximum at  $y=25\text{mm}$ . The variation of Shear Stress  $\tau_{zx}$  with the width is shown in Fig.6. We see that the shear stress for  $\theta = 0^\circ, 30^\circ$  and  $45^\circ$  increases rapidly up to width of 5mm, after which the variation in Shear Stress  $\tau_{zx}$  is slow. The Shear Stress drops when the width further increases i.e. beyond 20mm. The non-linear variation of the Shear Stress for  $\theta = 60^\circ$  is shown, with minimum stress at  $y=0\text{mm}$  and maximum stress at  $y=17.5\text{mm}$ . For  $\theta = 90^\circ$ , there is no significant variation of stress between  $y=5\text{mm}$  and 20mm, at the ends decrease in Stress value followed by an increase.

In most of the above cases, it is observed that the stresses are maximum near the ends of the plate in the width direction. This may be due to the interlaminar effect in addition to the coupling effect. The stresses shown in Figs. 5.8 - 5.10 are measured at the locations where the normal and shear stresses are maximum in the top interface of the adherend and adhesive.

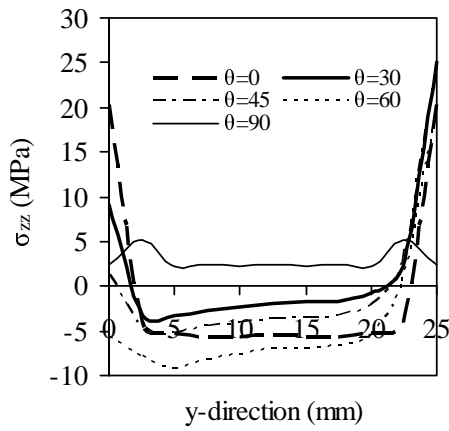


Figure 4: Variation of  $\sigma_{zz}$  across width.

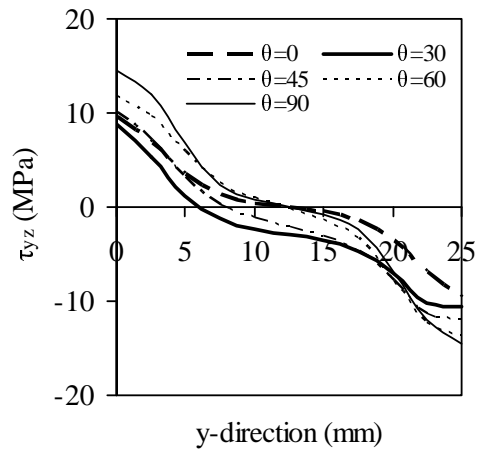


Figure 5: Variation of  $\tau_{yz}$  across width.

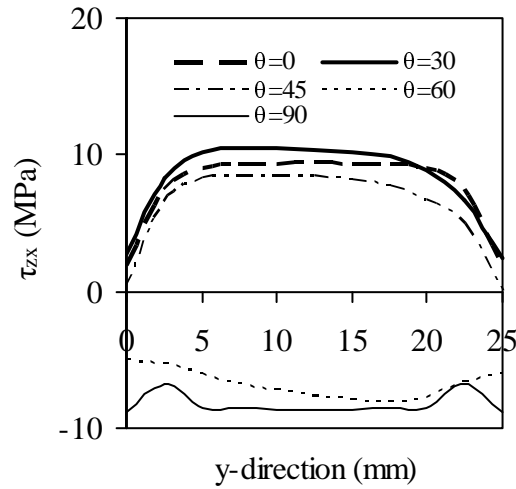


Figure 6: Variation of  $\tau_{zx}$  across width.

### Variation of the maximum stresses with respect to the fiber angle $\theta$

Load transfer between adjacent layers in a fiber-reinforced laminate takes place by means of interlaminar stresses, such as  $\sigma_{zz}$ ,  $\tau_{zx}$ , and  $\tau_{yz}$ . The principal reason for the existence of interlaminar stresses is the mismatch of Poisson's ratios  $\nu_{xy}$  and coefficients of mutual influence and between adjacent laminae. If the laminae were not bonded and could deform freely, an axial loading in x-direction would create dissimilar transverse strains  $\epsilon_{yy}$  in various laminae because of the difference in their Poisson's ratios. However, in perfect bonding, transverse strains must be identical throughout the laminate. The constraint against free transverse deformations produces normal stress  $\sigma_{yy}$  in each lamina and interlaminar shear stress  $\tau_{yz}$  at the lamina interfaces. Similarly, the difference in the coefficients of mutual influence would create dissimilar shear strains  $\gamma_{xy}$  in various laminae only if they were not bonded. For a bonded laminate, equal shear strains for all laminae require the development of

interlaminar shear stress  $\tau_{zx}$ . Although the force equilibrium in the y-direction is maintained by the action of  $\sigma_{yy}$  and  $\tau_{yz}$ , the force resultants associated with  $\sigma_{yy}$  and  $\tau_{yz}$  are not collinear. The moment equilibrium about the x-axis is satisfied by the action of the interlaminar normal stress  $\sigma_{zz}$  [22]. In addition the mismatch of coefficients of thermal expansion will also causes for the interlaminar stresses in thermal loading. In general case of loading the interlaminar stresses will be developed due to all of the above reasons. As the fiber angle  $\theta$  increases the mismatch in the poisons ratios of adherend and adhesive decreases up to certain angle and later increases, and the same trend can be expected in the variation of inter laminar stresses with respect to fiber angle. The effect of coefficients of mutual influence is to raise the stresses up to certain value of  $\theta$  and later the stresses decrease.

As the fiber angle  $\theta$  varies from  $0^0$  to  $90^0$ , the mismatch between the coefficients of thermal expansion of adherend and adhesive increases resulting in increase in stresses with respect to  $\theta$ . As the force transmission takes place through the interlaminar stresses from the adherend to adhesive, the stresses at the mid plane of adhesive will also be affected by the fiber angle.

Fig.7 illustrates the variation of normal stress  $\sigma_{zz}$  with fiber angle  $\theta$  on various surfaces. This stress on mid and top surfaces is increasing gradually with the increase of fiber angle up to  $30^0$  and  $37.5^0$  respectively, later the stress decreases. The increase of stress on these surfaces is due to the resultant influence of mismatch in  $\alpha$  and effect of mutual influence than the mismatch in  $\nu$ . The decrease in normal stress after some value of  $\theta$  in the above cases is due to mutual influence. The magnitude of normal stress variation on bottom interface is very less with the increase of fiber angle. Slight variation of stress between  $0^0$  and  $15^0$  is noticed due to mismatch in the coefficients of thermal expansion and effect of mutual influence of adhesive and adherend. Beyond  $15^0$ , i.e. between  $15^0$  and  $30^0$ , there is a small dip due to decrease of mismatch in poison's ratios of adherend and adhesive, followed by slight increase, slight decrease in stress with the increase of fiber angle.

Fig.8 depicts the variation of shear stress  $\tau_{yz}$  with fiber angle on various surfaces. This stress on top interface, minimum at  $\theta = 0^0$  and maximum at  $\theta = 75^0$ , is increasing with the increase of fiber angle up to  $75^0$  followed by drop in stress. Increase of stress up to  $75^0$  is due to the effect of mismatch in  $\alpha$  and effect of mutual influence, decrease of stress later due to effect of mutual influence. This stress on mid surface is minimum at  $\theta = 90^0$  and maximum at  $\theta = 37.5^0$ . The increase of stress up to  $37.5^0$  on mid surface is due to  $\alpha$  and mutual influence and decrease of stress beyond  $37.5^0$  is due to mutual influence.

Slight variation of shear stress  $\tau_{yz}$  on bottom interface is noticed up to  $\theta = 45^0$  because of influence of  $\alpha$  and mutual influence followed by a dip between  $45^0$  and  $60^0$  which is due to the reduction of mismatch in poisons ratio of adhesive and adherend. Later slight increase in stress up to  $90^0$  because of  $\alpha$  and poisons ratio.

The predicted shear stress  $\tau_{zx}$  verses fiber angle  $\theta$  curves of various surfaces is shown in Fig.9. The shear stress on mid surface is increasing linearly up to  $\theta = 30^0$  because of mismatch in coefficients of thermal expansion and effect of mutual influence followed by a dip between  $30^0$  and  $45^0$  due to reduction of mismatch in poisons ratio of adhesive and adherend. Later increase of stress is due to resultant

influence of mismatch in poisons ratio and coefficient of thermal expansion. This stress on mid surface is minimum at  $\theta = 0^0$  and maximum at  $\theta = 90^0$ . This stress on top inter face goes on increasing, reaches to their respective maxima at  $\theta = 30^0$  and decreases later with increase in fiber angle. The increase in stress is due to effect of mutual influence and mismatch in coefficient of thermal expansion, the decrease of stress is due to effect of mutual influence. On bottom interface, this stress decreases up to  $30^0$  due to poisons ratio effect later increasing up to  $75^0$  followed by drop in stress.

Fig.10 shows the variation of transverse deflection ‘w’ with respect to fiber angle  $\theta$ . The value of ‘w’ increases up to  $\theta = 30^0$ , decreases between  $30^0$  and  $60^0$  followed by an increase. The factors influencing the deflection are variation of stiffness and mutual influence with  $\theta$ .

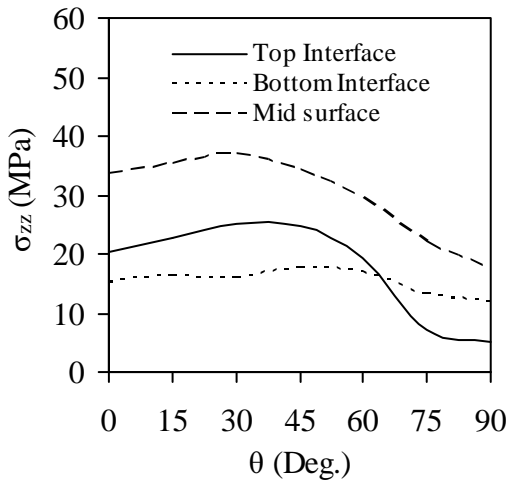


Figure 7: Variation of  $\sigma_{zz}$  with  $\theta$ .

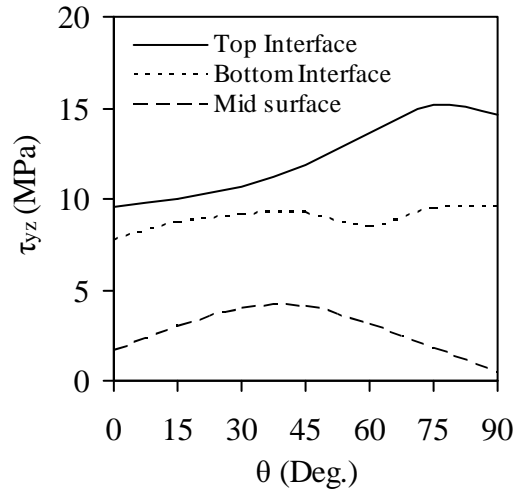


Figure 8: Variation of  $\tau_{yz}$  with  $\theta$ .

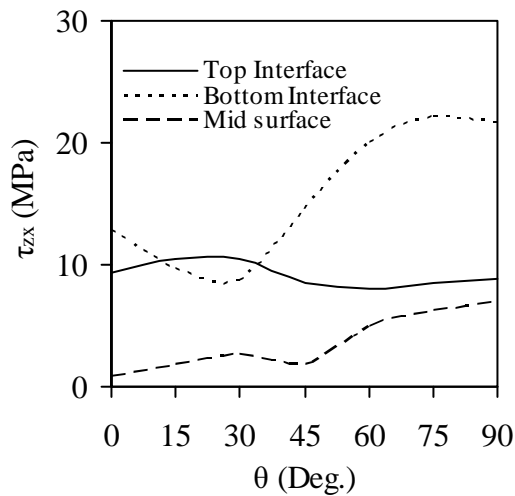


Figure 9: Variation of  $\tau_{zx}$  with  $\theta$ .

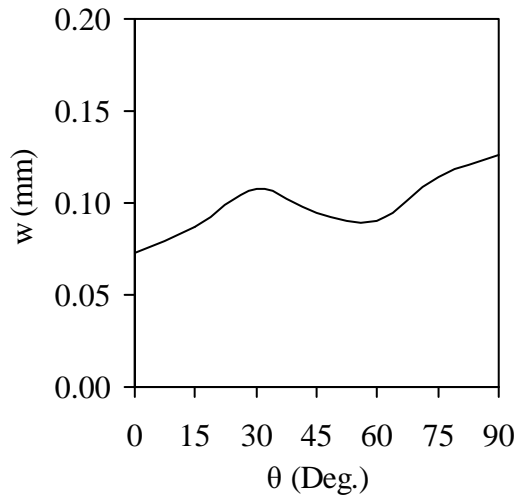


Figure 10: Variation of ‘w’ with  $\theta$ .

## Conclusions

Three-dimensional finite element analysis has been taken up for the evaluation of the interlaminar stresses at the interfaces of the adherends and adhesive, and the out-of-plane stresses at the middle surface of single lap joint made of FRP laminates of generally orthotropic nature subjected to non-linear temperature load. The following conclusions are drawn:

- Variation of the stresses in the width direction is significant and therefore three-dimensional analysis is necessary.
- It is observed that the peel stress intensity is more on mid surface between  $30^{\circ}$  and  $60^{\circ}$  resulting in cohesive failure of adhesive. Very less intensity of peel stress is noticed between  $75^{\circ}$  and  $90^{\circ}$ , hence higher fiber angles are suitable to avoid failure.
- The fiber angle  $\theta$  influences the stresses due to the mismatch in layer properties at the interfaces leading to delamination.

## References

- [1] Volkersen, O., 1938, "Die Niekraftverteilung in Zugbeanspruchten mit Konstanten Laschenquerschnitten. Luftfahrtforschung", 15, pp. 41–47.
- [2] Goland, M. and Reissner, E., 1944, "The Stresses in Cemented Joints", ASME Trans., Journal of Applied Mechanics, 11. pp.17–27.
- [3] Oplinger, D. W., 1991, "A Layered Beam Theory for Single Lap Joints", Army Materials Technology Laboratory Report, MTL TR91–23.
- [4] Hart-Smith, L. J., 1973, "Adhesive-Bonded Single Lap Joints", NASA-CR-112236.
- [5] Hart-Smith, L. J., 1973, "Adhesive-bonded Double Lap Joints", NASA-CR-112235.
- [6] Tsai, M. Y., Oplinger, D. W. and Morton, J., 1998, "Improved Theoretical Solutions for Adhesive Lap Joints", Int. Journal of Solids Structures, 35(13), pp.1163–1185.
- [7] Klarbring, A. and Movchan A.B., 1988, "Asymptotic modeling of adhesive joints", Mechanics of materials, 28, pp.137-145.
- [8] Kim H. and Kedward K., 2001, "Stress analysis of adhesively bonded joints under in plane shear loading", J. Adhesion, 76, pp.1-36
- [9] Penado F.E. and Dropek R.K., 1990, "Numerical design and analysis", Engineered materials Hand book, 3, Adhesives and Sealants, ASM International.
- [10] Tessler, A., Dambach M.L. and Oplinger D. W., 2000, "Efficient adaptive mesh refinement modeling of adhesive joints", presented at the work shop on bonded joints and assemblies in aircraft, ASTM/ASC, Texas A&M
- [11] Adams, R. D. and Peppiatt, N. A., 1974, "Stress Analysis of Adhesively Bonded Lap Joints", Journal of Strain Analysis, 9, pp.185–196.

- [12] Kairouz, K. C. and Matthews, F. L., 1993, “Strength and Failure Modes of Bonded Single Lap Joints between Cross-Ply Adherends”, *Composites*, 24(6), pp.475–484.
- [13] Tong, L. and Steven, G. P., 1999, “Analysis and Design of Structural Bonded Joints”, Kluwer Academic Publishers.
- [14] Li, Gang and Lee-Sullivan, Pearl, 2001, “Finite Element and Experimental Studies on Single-lap Balanced Joints in Tension”, *Int. Journal of Adhesion and Adhesives*, 21(3), pp. 211–220.
- [15] Delale, F., Erdogan, F. and Aydinoglu, M. N., 1982, “Stresses in Adhesively Bonded Joints: A Closed-form Solution”, *Journal of Composite Materials*, 15, pp.249–271.
- [16] Mortensen, F. and Thomsen, O. T., 2002, “Analysis of Adhesive Bonded Joints: A Unified Approach”, *Composite Science and Technology*, 62(7–8), pp.1011–1031.
- [17] Panigrahi, S. K. and Pradhan, B., 2007, “Three dimensional Failure analysis and damage Propagation behavior of Adhesively bonded Single lap joints in laminated FRP Composites”, *Journal of Reinforced plastics and Composites*, 26(2), pp.183-201.
- [18] Venkateswara Rao, M., Mohana Rao, K., Rama Chandra Raju, V., Bala Krishna Murthy, V. and Sridhara Raju, V.V., 2007, “Three-Dimensional Finite Element Analysis of Adhesively Bonded Single Lap Joints in Laminated FRP Composites”, *International Journal of Materials Sciences*, 2(3), pp. 309–319.
- [19] Venkateswara Rao, M., Mohana Rao, K., Rama Chandra Raju, V., Bala Krishna Murthy, V. and Sridhara Raju, V.V., 2007, “Analysis of Adhesively Bonded Single Lap Joints In Laminated FRP Composites subjected to Transverse Load”, Accepted for publication in *International Journal of Mechanics and Solids*.
- [20] ANSYS reference manuals (2006).
- [21] Tungikar VB, and Rao KM., 1994, “Three dimensional exact solution of thermal stresses in rectangular composite laminate”, *Composite Structures*, 27, pp.419-430.
- [22] Mallick, P. K., 1988, “Fiber-Reinforced Composites “, MARCEL DEKKER, INC., pp.159-162.

